Available online at www.sciencedirect.com
SCIENCE DIRECT®
Experimental Neurology 190 (2004) 276–288
Experimental Neurology
www.elsevier.com/locate/yexnr

# CNS stem and progenitor cell differentiation into functional neuronal circuits in three-dimensional collagen gels

W. Ma,[a,*] W. Fitzgerald,[b] Q.-Y. Liu,[c] T.J. O'Shaughnessy,[a] D. Maric,[d] H.J. Lin,[a] D.L. Alkon,[c] and J.L. Barker[d]

[a] *Center for Bio/Molecular Science and Engineering, Naval Research Laboratory, Washington, DC 20375, USA*
[b] *NASA-NIH Center for 3D Tissue Culture, National Institute of Child Health and Human Development, NIH, Bethesda, MD 20892, USA*
[c] *Blanchette Rockefeller Neuroscience Institute, Rockville, MD 20850, USA*
[d] *Lab of Neurophysiology, National Institute of Neurological Disorders and Stroke, NIH, Bethesda, MD 20892, USA*

Received 19 June 2003; revised 22 October 2003; accepted 31 October 2003
Available online 17 January 2004

**Abstract**

The mammalian central nervous system (CNS) has little capacity for self-repair after injury, and neurons are not capable of proliferating. Therefore, neural tissue engineering that combines neural stem and progenitor cells and biologically derived polymer scaffolds may revolutionize the medical approach to the treatment of damaged CNS tissues. Neural stem and progenitor cells isolated from embryonic rat cortical or subcortical neuroepithelium were dispersed within type I collagen, and the cell–collagen constructs were cultured in serum-free medium containing basic fibroblast growth factor. The collagen-entrapped stem and progenitors actively expanded and efficiently generated neurons, which developed neuronal polarity, neurotransmitters, ion channels/receptors, and excitability. $Ca^{2+}$ imaging showed that differentiation from $BrdU^{+}/TuJ1^{-}$ to $BrdU^{-}/TuJ1^{+}$ cells was accompanied by a shift in expression of functional receptors for neurotransmitters from cholinergic and purinergic to predominantly GABAergic and glutamatergic. Spontaneous postsynaptic currents were recorded by patch-clamping from precursor cell-derived neurons and these currents were partially blocked by 10-μM bicuculline, and completely blocked by additional 10 μM of the kainate receptor antagonist CNQX, indicating an appearance of both GABAergic and glutamatergic synaptic activities. Staining with endocytotic marker FM1-43 demonstrated active synaptic vesicle recycling occurring among collagen-entrapped neurons. These results show that neural stem and progenitor cells cultured in 3D collagen gels recapitulate CNS stem cell development; this is the first demonstration of CNS stem and progenitor cell-derived functional synapse and neuronal network formation in a 3D matrix. The proliferative capacity and neuronal differentiating potential of neural progenitors in 3D collagen gels suggest their potential use in attempts to promote neuronal regeneration in vivo.


*Keywords:* Neural stem cells; Proliferation; Neurogenesis; 3D matrix; Collagen; GABA; Glutamate; Acetylcholine; Synapse formation; $Ca^{2+}$ imaging

## Introduction

Functional recovery following brain and spinal cord injuries and neurodegenerative diseases is likely to require the transplantation of exogenous neural cells and tissues, since the mammalian central nervous system (CNS) has little capacity for self-repair. However, neural cell or tissue transplantation is limited by the lack of tissue donors and the low survival rate of grafted cells. There is a critical need for an alternative strategy for building biological substitutes, such as a three-dimensional (3D) culture of neural cells to repair or replace the function of damaged nerve tissues. Tissue engineering that combines neural cells and polymer scaffolds may generate functional 3D constructs to serve as replacement tissues or organs (Bellamkonda et al., 1998; Woerly et al., 1999). Since neurons are not capable of proliferating and neurons in culture are short-lived, there remain significant challenges for neural tissue engineering. Recent advances in neural progenitor cell biology show that progenitors can be isolated from the embryonic or adult CNS and placed in culture, where they are highly proliferative and differentiate into neurons and glial phenotypes (Gage, 1998, 2000; Li et al., 2001; Ma et al., 1998, 2000;

* Corresponding author. Center for Bio/Molecular Science and Engineering, Code 6900, Naval Research Laboratory, 4555 Overlook Avenue SW, Washington, DC 20375. Fax: +1-202-767-9598.
*E-mail address:* wma@cbmse.nrl.navy.mil (W. Ma).

0014-4886/$ - see front matter © 2004 Elsevier Inc. All rights reserved.
doi:10.1016/j.expneurol.2003.10.016

Maric et al., 2000a; McKay, 1997). Therefore, CNS progenitors have potential to be a valuable source of a specific neural cell type, representing an ideal cell type for the neural tissue engineering (Fisher, 1997; Gage et al., 1995).

Polymer scaffolds play a critical role in neural tissue engineering, since neural progenitors and progeny like most other mammalian cells are anchorage-dependent and require the attachment to a solid surface (Ruoslahti, 1997). In the CNS, neural cells adhere to the fibrillar protein meshwork known as the extracellular matrix (ECM). Dynamic cell–ECM interactions trigger specific cell signaling and maintain proper cell growth, differentiation, and survival. A loss of the cell–ECM contacts may cause cell apoptosis (Ruoslahti, 1997). In the ECM, there is a microenvironment (niche), in which extrinsic signals such as ECM proteins and soluble factors from other cells control progenitor cell proliferation and fate (Watt and Hogan, 2000). Thus, proper design of scaffold matrices may allow them to mimic the native ECM and to contain necessary extrinsic factors for generating neural tissues from progenitor cells in an in vitro system. Therefore, the reconstruction of ECM equivalents in polymer scaffolds may play a central role in tissue engineering. Among polymer scaffolds, hydrogels are attractive because of their highly porous and hydrated structure that both allow cells to assemble spontaneously into tissue architecture and the infusion of nutrients and oxygen into, and exit of waste products and $CO_2$ out of the cells. In the present study, collagen was chosen because collagen is a biologically derived hydrogel and the major class of insoluble fibrous protein in the ECM. We have previously demonstrated that neural progenitor cells isolated from embryonic rat CNS tissue rapidly proliferate and differentiate into neurons and astrocytes in type I collagen gels (O'Connor et al., 2000). It is unknown whether or not the collagen-entrapped neural progenitors are able to differentiate into excitable neurons that form synapses and functional neuronal circuits and networks. Synapse formation is required in the development of functional neuronal networks where neurons communicate and influence other neurons. The present study explored the ability of a 3D collagen matrix to support neural progenitor proliferation and differentiation in vitro. In response to collagen and bFGF, the collagen-entrapped neural progenitor rapidly expanded and spontaneously differentiated into excitable neurons and formed synapses. Such progenitor cell–collagen constructs may be particularly useful as engineered nerve tissue replacement for brain or spinal cord injury and damaged tissue in neurodegenerative diseases.

## Materials and methods

### *Preparation of cell–collagen constructs and maintenance in culture*

Cell–collagen constructs were prepared as described previously (O'Connor et al., 2000). Briefly, collagen (Rat tail tendon, Type I, Boehringer Mannheim Corp., Indianapolis, IN), purchased as a sterile, lyophilized powder, was dissolved to a final concentration of 3 mg/ml by addition of sterile 0.2% v/v acetic acid (pH 3–4). To prepare gels, the collagen solution was diluted with an equal volume of 2× phosphate-buffered saline (PBS, Gibco) and an amount of cell media to achieve a final collagen concentration of 0.5 mg/ml (maintaining physiological osmolarity, 250–300 mOsM). After adjusting the pH of the collagen solution to pH 7.4 by the addition of 1 N NaOH, the solution was chilled in an ice bath to prevent gel formation. Cells were added at the desired density, along with more cell media, if necessary, to obtain a final collagen concentration of 0.4 mg/ml. The cell–collagen solution was allowed to warm at room temperature and after approximately 10 min, 0.4 ml aliquots of the collagen–cell suspension were placed into wells of 24-well tissue culture plates. The gels were placed in an incubator (37 °C, 5% $CO_2$, 20% $O_2$, 99% Rh) for 1–2 h to allow gel formation. Once the gel had set, 0.5 ml of cell media was added to the top of the gels and the matrix was returned to the incubator. Neural progenitor cells were immobilized by preparing a suspension of cells in a pre-gel solution of collagen at a cell density of $2 \times 10^5$/ml. The cells were cultured in gels while exchanging the culture media every 3–4 days. All trials were carried out at least in triplicate.

### *Live/Dead staining*

Cell viability was determined by staining immobilized cells with Live/Dead Viability/Cytotoxicity Kit (Molecular Probes, Eugene, OR). Staining procedures were previously described (O'Connor et al., 2000). The kit contains two fluorescent probes that measure cell viability. Live cells are stained with green fluorescence due to the enzymatic conversion of the nonfluorescent, cell-permeant dye calcein AM to the intensely fluorescent calcein (ex/em approximately 495/515 nm). Dead cells are identified by staining with ethidium homodimer (EthD-1), which enters cells with damaged membranes, and upon binding to nucleic acids, produces a bright red fluorescence (ex/em approximately 495/635). EthD-1 is excluded by the intact plasma membrane of live cells. Live/dead stain was prepared with 2 μM calcein AM and 4 μM EthD-1 in PBS. For assessment of immobilized cells, 0.2 ml of the dye solution was added to 0.4-ml gel samples along with 0.2 ml of NB/B27. The samples were incubated with the dyes for 1 h after which the excess dye solution was removed and 0.5 ml of fresh PBS was added for 30 min. For imaging, excess buffer was removed to stabilize the gel sample. Images were captured via the Leica confocal microscopy system described later.

### *Immunocytochemistry*

#### *Double-immunostaining for BrdU and TuJ1*

To identify differentiating neurons derived from proliferating progenitor cells, cell cultures were double-immu-

nostained for BrdU and neuron-specific β-tubulin (TuJ1) (Lee et al., 1990; Menezes and Luskin, 1994). Ten-micromolar BrdU was included for the last 4 h before fixation with 70% ethanol. Cells incorporating BrdU were identified using the FITC-conjugated mouse Class $IgG_1$ anti-BrdU (1:50, Becton Dickinson, Mountain View, CA). Differentiating neurons were revealed using a monoclonal mouse Class $IgG_{2a}$ anti-TuJ1 antibody (1:1,000). Secondary antibody was rhodamine-conjugated donkey anti-mouse $IgG_{2a}$ (1:50, Southern Biotechnology Associates, Inc., Birmingham, AL). The distribution of $BrdU^+$ and $TuJ1^+$ cells was examined under a Nikon epifluorescence or a Leica confocal microscope.

*Double-immunostaining for BrdU and GFAP or O4*

To evaluate possible differentiation of neural progenitor cells along glial lineages, cell cultures were double-immunostained for BrdU and astrocytic marker glial fibrillary acidic protein (GFAP) or O4 (a marker for oligodendrocyte lineage). Ten μM BrdU was included for the last 4 h before fixation with 70% ethanol. $BrdU^+$ cells were identified by FITC-conjugated mouse Class $IgG_1$ anti-BrdU. Astrocytes and oligodendrocytes were detected by rabbit polyclonal anti-GFAP (1: 500, Chemicon, Temecula, CA) and mouse monoclonal antibody O4 (1:100, Boehringer Mannheim), respectively, followed by an incubation with rhodamine-conjugated donkey anti-rabbit IgG or donkey anti-mouse IgM (Jackson Immunological Research, West Grove, PA).

*Double-immunostaining for BrdU and GABA, glutamate or TH*

To detect differentiated neurons expressing neurotransmitters GABA, glutamate and dopamine, cultures were exposed to 10 μM BrdU for 4 h and then fixed with 70% alcohol followed by 2% paraformaldehyde in 0.1 M phosphate buffer, pH 7.4. Cells were incubated overnight with mouse anti-bromoceoxyuridine (BrdU) and rabbit anti-GABA (Chemicon), rabbit anti-glutamate (Chemicon), or rabbit anti-dopamine synthetic enzyme, tyrosine hydroxylase TH (Chemicon), followed by incubation with a mixture of rhodamine-conjugated donkey anti-rabbit IgG and FITC-conjugated donkey anti-mouse IgG (Jackson Immunological Research) for 45 min.

*Double-immunostaining for MAP2 and NF150*

To characterize the polarity of progenitor cell-derived neurons, cells were double-immunostained for MAP2 and NF150. Cultures were fixed for 20 min in 4% formaldehyde in PBS before exposure to mouse monoclonal anti-MAP2 antibody (1:100, Sigma, St. Louis, MO) and rabbit polyclonal anti-neurofilament 150 (NF150) (1:250, Chemicon) overnight. Secondary antibody solution was a mixture of rhodamine-conjugated donkey anti-rabbit IgG and FITC-conjugated donkey anti-mouse IgG (Jackson Immunological Research) for 45 min.

*Immunocytochemistry for pre- and postsynaptic specializations*

Staining procedures were as described previously (Ma et al., 1998). 3D cell–collagen gels were rinsed in phosphate-buffered saline (PBS) and fixed with 4% formaldehyde in 0.1 M phosphate buffer (pH 7.0) for 30 min at room temperature and rinsed in PBS. Cells were exposed to a mixture of rabbit polyclonal anti-synapsin I (1:500) (Chemicon) and monoclonal anti-MAP2 (1:300) (Sigma) overnight at 4°C. MAP-2 is a well-established marker for the identification of neuronal cell bodies and dendrites. After exposure to primary antibodies, the cells were rinsed in PBS and incubated for 45 min at room temperature with a mixture of rhodamine-conjugated donkey anti-rabbit IgG and fluorescein-conjugated donkey anti-mouse IgG (1:50) (Jackson Immunological Research). After rinses in PBS, cultures were photographed under phase-contrast and epifluorescence or confocal microscope optics (Leica TCS NT, Leica Microsystems, Heidelberg, Germany). Negative controls with omission of primary antibodies were run simultaneously.

*Confocal imaging*

Images of stained cells were captured via confocal laser scanning microscopy using a spectral confocal microscope (Leica TCS NT, Leica Microsystems). Collagen gel samples were placed in glass bottom 35-mm culture dishes for imaging. Sections of the gels, approximately 1000 × 1000 × 500 μm, were scanned using a 20×/0.40 dry plan lens. Excitation wavelength was provided at 488 nm from an argon laser and at 568 nm from a krypton laser. The region of interest in the gel sample was identified and the system software was programmed to collect images at 10-μm intervals through the thickness of the gel (z-dimension). Projected images created by superimposing the series of images captured stepwise at different planes through the gel sample onto one plane are presented in Fig. 2. Proliferating and total cells on each plane were quantified by counting the number of $BrdU^+$ and $PI^+$ cells in five regions taken at random for each gel sample. Three separate immobilization trials were performed using freshly isolated cells. Counting was completed using Scion Image software (PC version of NIH image, Scion Corporation, Frederick, MD) which allowed $BrdU^+$ (green) cells to be separated from the $PI^+$ (red) cells.

*$Ca^{2+}$ imaging*

Cell–collagen constructs cultured for 3, 7, 14, and 21 days were loaded with 2 μM fluo-3 AM (Molecular Probes) for 1 h at 37°C. At the end of the incubation, the cells were rinsed in normal physiological medium (in mM): 145 NaCl, 5 KCl, 1.8 $CaCl_2$, 0.8 $MgCl_2$, 10 HEPES, 10 glucose (pH 7.4, osmolarity 290 mOsM). Fluo-3-loaded cells were recorded using the Zeiss Attofluor Ratio Vision workstation

(Atto Instruments, Rockville, MD) equipped with an Axiovert 135 inverted microscope (Carl Zeiss, Thornwood, NY) and an ICCD camera (Atto Instruments). The fluo-3 dye was sequentially excited at 500-ms intervals with a 100-W mercury arc lamp filtered at 488 + 5 nm and the corresponding emissions acquired through a 510-nm dichroic mirror and 520 nm long-pass filter set. All filters were obtained from Chroma Technology Corp., Brattleboro, VT. To collect fluo-3 fluorescence signals, regions of interest (ROI) were drawn electronically around individual cells in the recording field. The fluorescence intensities from up to 99 ROIs were digitized simultaneously with a matrix image processing board and plotted as line graphs using Attograph for Windows analysis software (Atto Instruments). Changes in $[Ca^{2+}]_c$ were monitored as changes in the relative fluorescence of fluo-3, where an increase in fluorescence intensity, measured in arbitrary fluorescence units (afu), reflected a proportional increase in $[Ca^{2+}]_c$ concentration. All measurements were performed at room temperature (22–24 °C).

*Patch clamp recording and data analysis*

To characterize ion currents of neural progenitor cells during their differentiation and to identify functional synaptic activity, we have carried out patch-clamp recordings from randomly selected neural progenitor cells and their progeny on collagen gels. Dissociated progenitor cells were seeded onto the partially formed collagen gels at a density of $2 \times 10^5$ cells/ml. Seeding onto partially formed gels ensured that a portion of the cells would be sufficiently close to the surface for patch clamp experiments. The final concentration of collagen in the gels was 0.4 mg/ml and the gels were cylindrical with a radius of 7 mm and depth of 3 mm. Neural progenitor cells and their progeny proliferated and apparently differentiated. Neurite outgrowth was evident in three directions. Whole-cell patch-clamping methods were performed as described by Hamill et al. (1981) in cells cultured for 5 and 14 days. Patch pipettes were pulled with a Narishige PP-83 two-stage puller and heat-polished with a CPM-2 microforge (Adams List Associates, Westbury, NY). The patch electrode resistance was 5–10 MΩ when filled with an intracellular solution containing (in mM): 50 KCl, 90 K-aspartate, 5 ethylene glycol-bis(*b*-aminoethyl ether)-*N*, *N*, *N*′, *N*′-tetraacetic acid (EGTA)-KOH, 5 *N*-[2-hydroxyethyl]-piperazine-*N*′-[2-ethanesulfonic acid] (HEPES), 5 MgATP, pH to 7.4 with KOH. The extracellular bathing solution contained (in mM): 140 NaCl, 5 KCl, 1.8 $CaCl_2$, 0.8 $MgCl_2$, 10 glucose, and 10 HEPES, pH to 7.4 with NaOH. After achieving the cell-attached patch clamp configuration, whole-cell recording was attempted only when the seal resistance exceeded 10 GΩ. An Axopatch 200B patch-clamp amplifier (Axon Instruments, Foster City, CA) coupled with pClamp and AxoTape (v6.0.4 and v2.0.2, respectively; Axon Instruments) data acquisition software was used for both current and voltage clamp recordings. Signals were filtered at 2–5 kHz with the patch amplifier's built-in four pole, Bessel low-pass filter and digitized at 10 kHz. All patch clamp experiments were conducted at room temperature (22–25 °C). Patching the cells in collagen gels presents several challenges not typically encountered in traditional 2D cultures. Firstly, the patch electrode does not effectively penetrate the collagen matrix, making it necessary to patch cells located at or near the surface of the gel. Seeding the cells onto partially formed gels produced a population of neurons at the surface of the gel, which were easily identified by adjusting the focal plane of the microscope. The second difficulty in patching neurons suspended in gels involves stabilizing the gel. The gels were placed in 35-mm petri dishes and secured with a slice anchor (Warner Instrument Corp., Hamden, CT) before the addition of 1 ml of bath solution. While this configuration held the gel steady enough for patching, seals were not as stable as typically obtained in 2D cultures of neurons. During recordings, cells were superfused continuously with a perfusion system at the rate of approximately 0.3–0.5 ml/min., which was controlled by the air pressure applied to the solution reservoir.

*Staining with endocytotic marker FM1-43*

To visualize pre-synaptic vesicle accumulations, cells were loaded with 10-μM styryl dye (*N*-3-triethylammonmpropyl)-4-(4-(dibutylamino) styryl) pyridinium dibromide (FM1-43) in depolarizing extracellular solution (50 mM $K^+$) at 37 °C. The cells were rinsed with normal physiological medium (see *$Ca^{2+}$ imaging*) without dye. Since the FM1-43 staining was performed under saturated conditions, the rate of endocytosis should not affect staining intensity. Cells were imaged with the Zeiss Attofluor Ratio Vision workstation (Atto Instruments) equipped with an Axiovert 135 inverted microscope (Carl Zeiss) and an ICCD camera (Atto Instruments). A subsequent application of depolarizing solution without FM1-43 resulted in a complete destaining of FM1-43 stained puncta.

## Results

*Neural progenitor cells actively expand within 3D collagen gels*

Neuroepithelial cells isolated from embryonic day 13 rat cerebral cortex or subcortical regions were immobilized by matrix entrapment in collagen gels (0.5 mg/ml). The pre-gel solution of cell–collagen was placed into a well plate and formed a disk-like gel 14 mm in diameter and 3 mm in height (Fig. 1a). As a result of cross-link formation, the cells were trapped within and scattered throughout the gel. The collagen-entrapped progenitors rapidly expanded in neurobasal/B27 medium containing bFGF. Phase-contrast photomicrographs of representative fields of cells in the cultures (Figs. 1b–f) at days 0 (b), 1 (c), 2 (d), 5 (e), and 7 (f) show

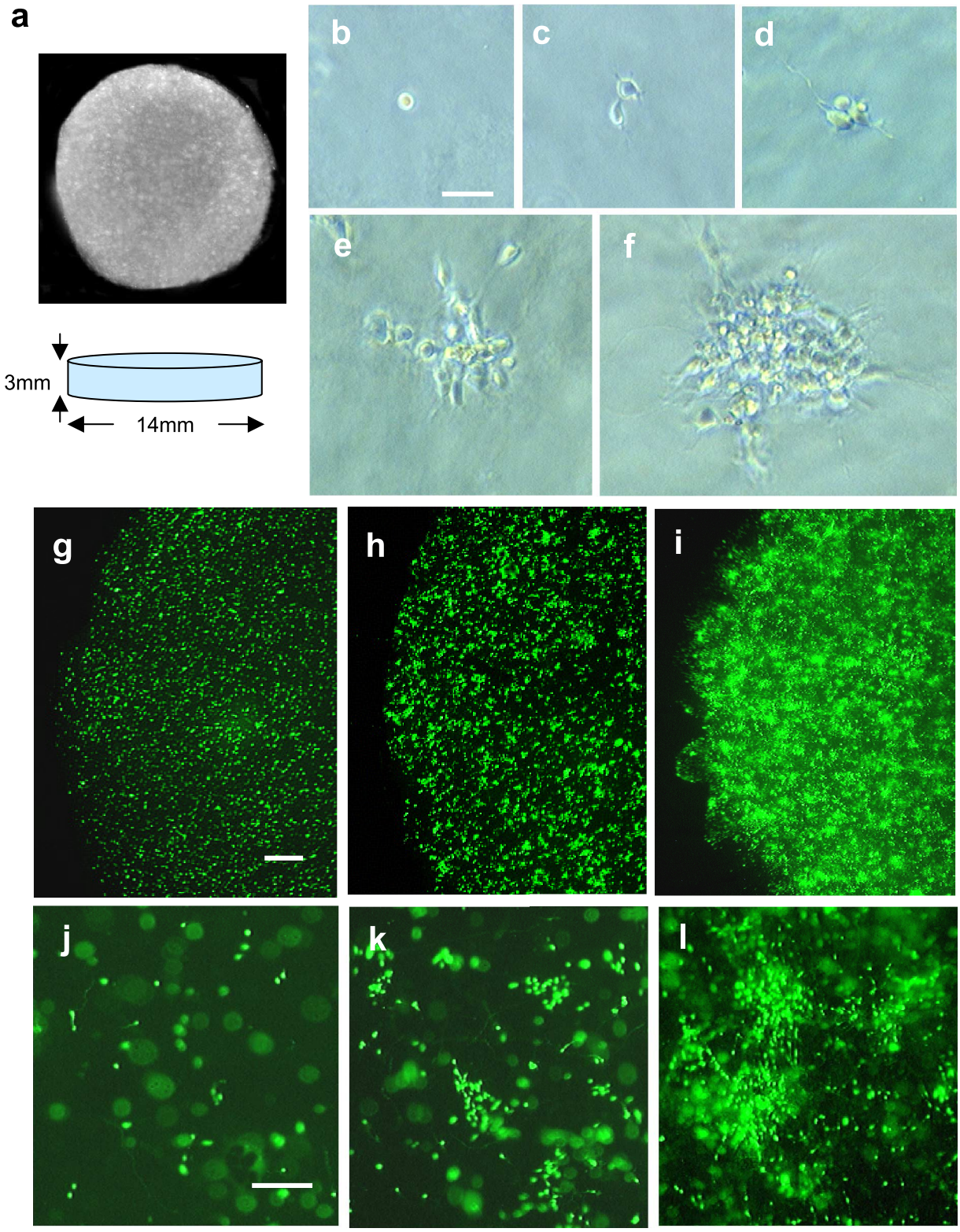


Fig. 1. Neural progenitor cells form clones of viable progeny entrapped in 3D collagen gels. (a) Neuroepithelial cells dissociated from cortical or subcortical regions at E13 were mixed with the collagen pre-gel solution and placed in an incubator for 1–2 h until the formation of a disk-like gel 14 mm in diameter and 3-mm deep. (b–f) Time-lapse phase-contrast micrographs of collagen-entrapped neural progenitor cells, which rapidly expanded from a single cell at the day of plating (b), to a clone-like cluster at day 5 (f). Photograph (c) was taken at day 1, (d) at day 2 and (e) at day 3. (g–i) Fluorescence micrographs of calcein staining of rapidly expanded neural progenitor cells from individual cells (g, at day 1) to clone-like clusters (h, at day 4 and i, at day 14). (j–l) Higher magnification of calcein-stained cells at day 1 (j), 4 (k) and 14 (l) showing a high viability of progenitor cells in 3D collagen since calcein stains only live cells. Scale bars in $b$ = 100 μm and applies to c–f; in $g$ = 500 μm applies to h–i; in $j$ = 300 μm and applies to k–l.

that suspended individual progenitor cells divided and over 1 week readily formed characteristic clone-like, multi-cellular clusters. The viability of the expanded neural progenitor cells was examined using Live/Dead viability staining. Low (Figs. 1g–i) and higher (Figs. 1j–l) magnifications of calcein staining, which stains only live cells and generates green fluorescence signals, show a rapid expansion and high viability of entrapped cells cultured in collagen gels for 1 (g and j), 4 (h and k) and 14 (i and l) days.

*Quantification of progenitor cell proliferation*

To quantify cell proliferation, changes in cell numbers indexed with propidium iodide (PI) that labels nuclei of all cells in the culture, and the number of actively proliferating (BrdU-incorporated) cells was counted. To examine changes in cell number from days 1 to 21 in culture, cells were released from the cell–collagen constructs by using collagenase, and $PI^+$ cells (red, Fig. 2a) were counted. As shown in Fig. 2b, the $PI^+$ cells in the 3D culture exhibited a growth pattern with several phases. In the first 1–2 days, no apparent increase in cell number was detected. A rapid 5-fold increase in the $PI^+$ cell number occurred between days 3 and 10. Shortly after a peak at day 10, the cell number entered a plateau phase with no further significant changes over the next week. A decline in the $PI^+$ cells was seen after 2 weeks in culture.

To quantify BrdU incorporation, the cell–collagen constructs cultured for 4, 14, and 21 days were incubated with BrdU for 4 h before being processed for BrdU immunocytochemistry (green). The cells were counterstained with PI (red). We indexed proliferation at different times by quantifying the proportion of $BrdU^+$ cells in terms of the total cell number identified with nuclear PI fluorescence. Projected images created by superimposing a series of images of $BrdU^+$ nuclei captured stepwise at different planes through the gel sample onto one plane are shown in Fig. 2a. Counting showed that proliferating cells rapidly increased from approximately 15% to 81% over the period of time from days 2 to 7 in culture (Fig. 2c). The index peaked over days 7–10 and then declined progressively over the next 2 weeks. Thus, evidence of BrdU incorporation began at day 2 before total cell number began to increase and peaked before cell number plateaued.

*Collagen-entrapped neural progenitor cell expression of neuronal markers*

Our previous work has shown that neural progenitor cells dissociated from embryonic cortices cultured on 2D PDL/fibronectin surface (Ma et al., 1998) and in 3D collagen gels differentiate into $TuJ1^+$ neurons (O'Connor et al., 2000). Little is known, however, about the extent to which progenitor cells in a 3D matrix can differentiate into neurons and

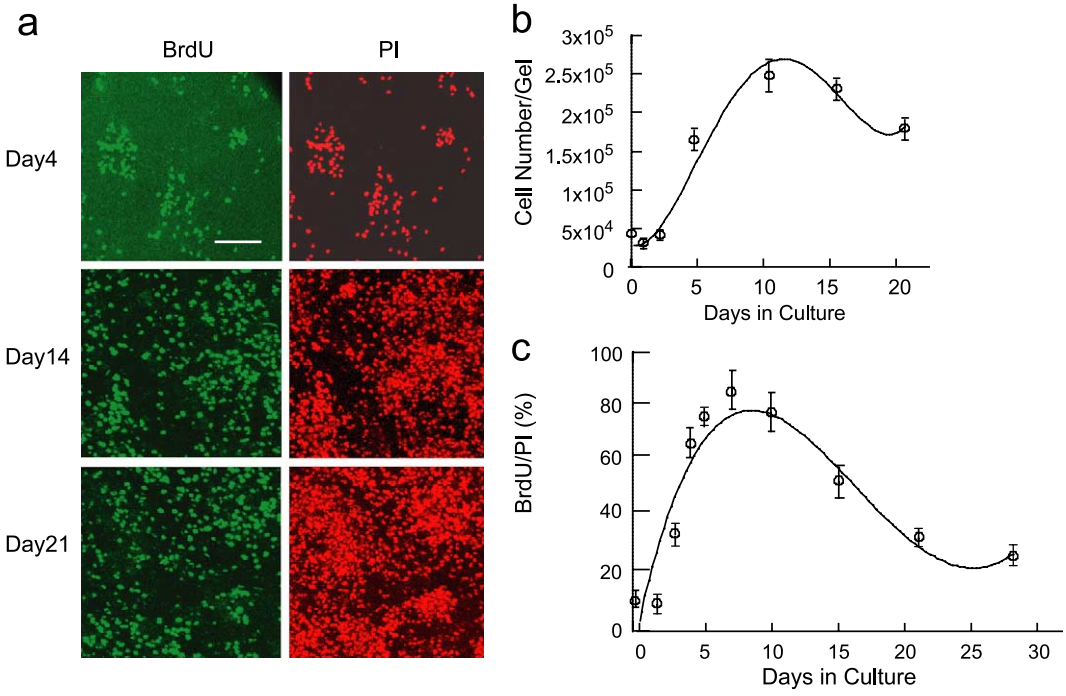


Fig. 2. Collagen-entrapped neural progenitor cells actively proliferate. (a) Confocal microscopic images of $BrdU^+$ cells and their counterstaining for PI at days 4, 14, and 21 in culture show the expansion of progenitors overtime. There is a higher percentage of $BrdU^+$ cells at the end of the first week and a decline in the $BrdU^+$ cell number at the end of the second and third weeks, while the total number of cells identified by $PI^+$ nuclei increases. (b) Time-course of progenitor cell expansion in 3D collagen gels. In the early phase, there is no apparent increase in cell number per gel until after day 2 in culture. The number of cell peaks at day 10 and declines in the second week. (c) Time-course of the proliferation index ($BrdU^+$ cell number divided by total number of $PI^+$ nuclei) from days 1 to 28 in culture. The index of proliferation first increases, then plateaus, and later decreases. Scale bar in *a* = 500 μm.

other neural cell types. We used immunocytochemistry with specific cell markers and demonstrated that collagen-entrapped progenitor cells cause all three major CNS cell types: neurons (Figs. 3c, g, red), astrocytes (Fig. 3e, red), and oligodendrocytes (Fig. 3f). Neurons were the first differentiated cells to arise autonomously. Second day following immobilization, a few TuJ1$^+$ neuronal cells appeared (Fig. 3c), while most of cells immunostained for BrdU (Fig. 3b) or nestin (Fig. 3d), an intermediate filament protein characteristic of neural precursor and progenitor cells (Lendahl et al., 1990). GFAP$^+$ (Fig. 3e) and O4$^+$ (Fig. 3f) cells did not appear until after 10 days in culture. To identify the pre- and post-mitotic stages of collagen-entrapped progenitor cells, we incubated them with BrdU for 4 h before fixing and staining. Double-immunostaining for BrdU and the neuronal marker TuJ1 showed that at day 1 in culture, most cells incorporated BrdU while TuJ1 immunoreactivity was barely detectable. Less than 1% of all cells were TuJ1$^+$. During the ensuing 2–3 days, as cells expanded into clone-like clusters, an increasing number of TuJ1$^+$ differentiating neurons with processes (about 4–6% TuJ1$^+$/BrdU$^-$ cells) were seen in a total of 354 cells. At day 5 in culture, about 9% cells were TuJ1$^+$/BrdU$^-$ in a total of 442 cells analyzed, while approximately 78% cells were BrdU$^+$. No glial cells were detected by anti-GFAP or anti-O4. In the cell–collagen constructs, proliferating cells were quite often in the core of clusters, while TuJ1$^+$ cells appeared at the periphery of a cell cluster (Figs. 3g, h). During the second week in culture, TuJ1$^+$ cells continued to increase and migrated out of the cores of the clusters until about day 14 when the relative proportion of BrdU$^+$ cells declined to about 51%, while the percentage of TuJ1$^+$/BrdU$^-$ neurons continued to increase to about 35% of a total of 743 cells analyzed (Fig. 3h). Many GFAP$^+$ astrocytes and O4$^+$ oligodendrocytes were detected throughout the gel at this time. It was clear that there was a gradual shift in cell phenotype entrapped in the gel from most neural progenitor cells beginning to proliferate in the first 5 days to a heterogeneous population, initially including neurons and later

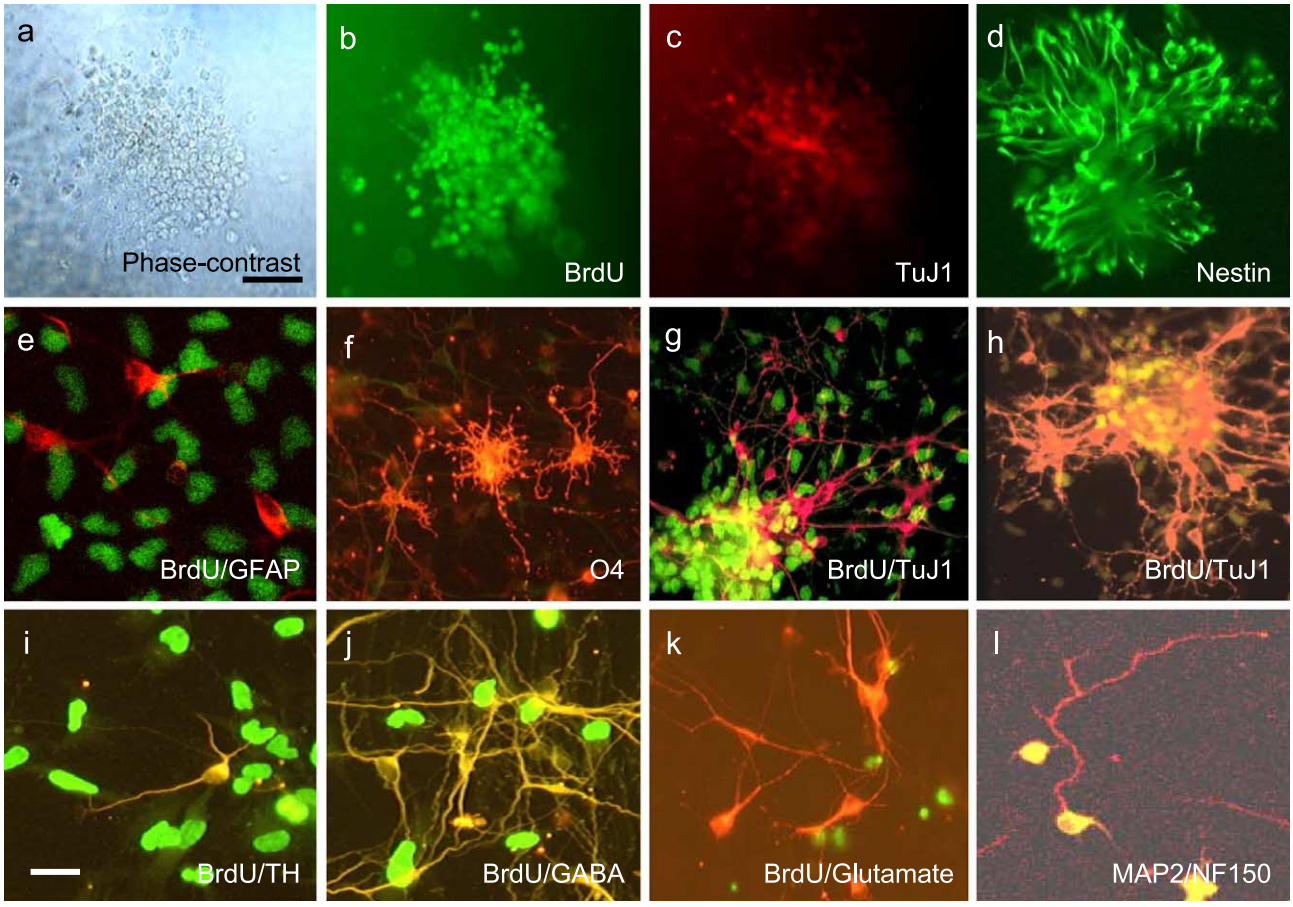


Fig. 3. Collagen-entrapped cortical or subcortical progenitor cells differentiate into neurons, astrocytes and oligodendrocytes. Progenitor cells were expanded in a collagen gel for 3, 5, 7, 14, and 21 days, then immunostained for neuronal (TuJ1) and glial (GFAP, O4) markers, BrdU, nestin, neurofilaments (MAP2/NF150) and neurotransmitters or enzymes (GABA, glutamate, tyrosine hydroxylase, TH). At day 5, many of the cells visualized in phase contrast (a) are actively proliferating (BrdU$^+$, b) and nestin$^+$ (d), but fewer are neuronal (TuJ1$^+$, c). At day 14 in culture, a variety of differentiated cells appear. At higher magnification (e–l), individual progeny can be identified that are GFAP$^+$ (e). Many cells are BrdU$^+$. Some cells are oligodendrocytes (O4$^+$, f). Cell migration occurs from a core of a proliferating cluster (BrdU$^+$, g, h). Some of neurons are TH$^+$ (i) and BrdU$^+$ while others are either GABA$^+$ (j) and BrdU$^+$ or glutamate$^+$ (k) and BrdU$^+$. Both dendrites (MAP2$^+$) and axon (NF150$^+$) are differentiated by neurons (l). Scale bar in *a* = 150 μm and applies to b–d; in *i* = 50 μm and applies to e–l.

astrocytes and oligodendrocytes in the second week. The expansion and sequential differentiation of neural progenitor cells in the 3D collagen gel closely paralleled that observed in 2D monolayer cultures on poly-D-lysine/fibronectin-coated surfaces (Ma et al., 1998; Maric et al., 2000a; O'Connor et al., 2000).

*Neural progenitor cell progeny displays neuronal polarity and neurotransmitters*

Neurons are highly polarized structurally and functionally as individual cells and as elements in a neuronal circuit. Naturally, neurons develop a single axon and multiple dendrites in the CNS and in vitro. Axons are specialized for neurotransmitter release whereas dendrites primarily express postsynaptic receptors for signal reception. To determine whether progenitor cell-derived neurons in 3D collagen gels develop normal neuronal polarity, double-immunostaining for 150-kDa neurofilament (NF150) and MAP2 was carried out. Since developing axons lack high concentrations of MAP2 (Bernhardt and Matus, 1984), and NF150 is in axons, dendrites, and cell bodies, those processes staining positive and negative for NF150 and MAP2, respectively, can be defined as axons (Stenger et al., 1998). Fig. 3l shows that each $MAP2^+$ cell body ($MAP2^+$, green) in gels gave rise to a single axon ($NF150^+$, red).

To examine the appearance of neurotransmitters in progenitor cell-derived neurons, immunostaining for GABA, glutamate, and dopamine-synthetic enzyme TH was carried out. In the first week of culture, a significant number of cells reacted to antibodies against GABA or glutamate (Figs. 3j, k). Some progeny of subcortical neuroepithelial founders were positive when stained with anti-TH (Fig. 3i). These results show that neurons differentially in the 3D gel exhibit morphological polarity and several neurotransmitters.

*A shift in cytosolic $Ca^{2+}$ responses from acetylcholine and ATP to predominantly GABA and glutamate during neural progenitor cell expansion and differentiation*

Results from double-immunostaining for BrdU and TuJ1 of 3D cultures (see above) have shown that the percentage of $TuJ1^+/BrdU^-$ neurons increased from about 9% at day 5 to about 35% at day 14 in culture, while proliferating ($BrdU^+/TuJ1^-$) cells decreased from approximately 78% at day 5 to 50% at day 14 in culture. The

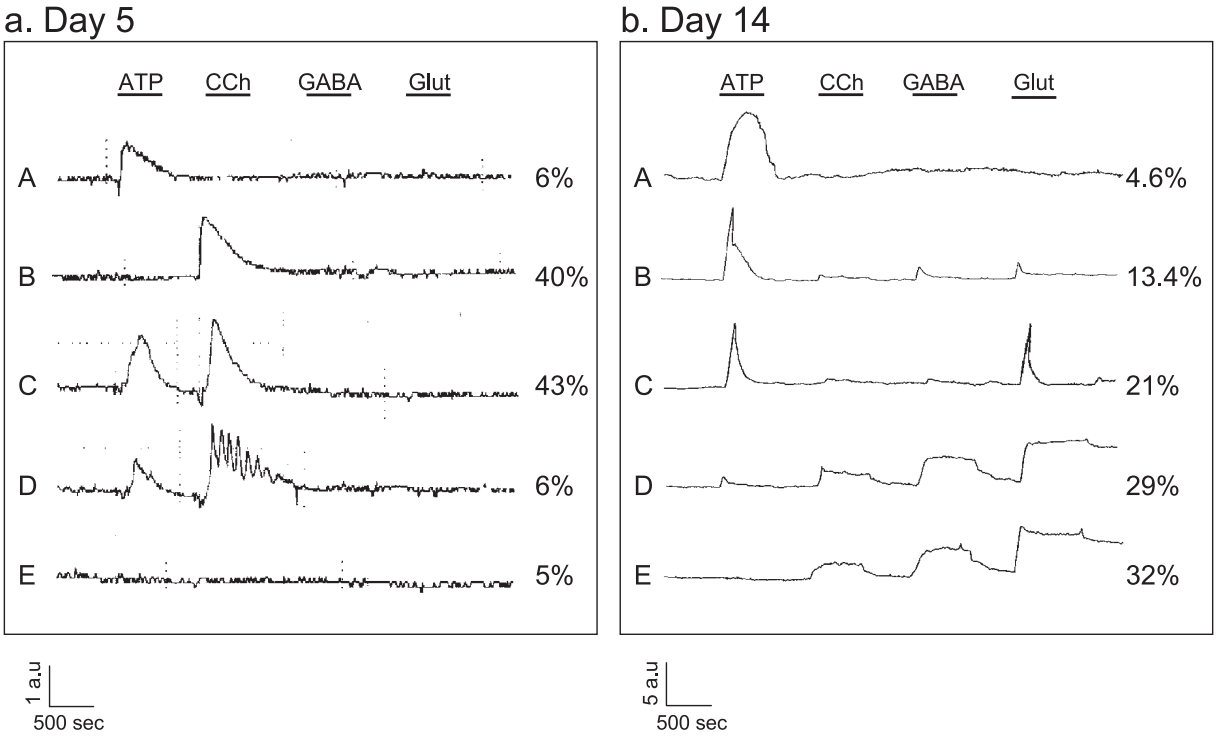


Fig. 4. Cytosolic $Ca^{2+}$ responses to neurotransmitters change in their cellular distribution during expansion and differentiation of progenitors. BrdU incorporation and immunocytostaining of progenitor cultures at days 5 and 14 for neural markers demonstrated a shift from undifferentiated to differentiated state. To characterize functional expression of neurotransmitter receptors during progenitor expansion and differentiation, $Ca^{2+}$ imaging was carried out at 5 days (a) and 14 days (b) in culture. The cells were loaded with fura-2 and were sequentially exposed to 1 mM ATP, 100 μM CCh, 10 μM GABA, and 50 μM glutamate with intervening washes between each application. (a) In 5-day-old cultures, 40% of the cells respond to CCh alone and 49% of cells respond to both ATP and CCh. None of the cells respond to GABA or glutamate. (b) In 14-day-old cultures, 61% of the cells respond to CCh, GABA and glutamate, while 39% of the cells respond to ATP. Since most post-mitotic neurons respond to ACh, GABA and glutamate (Maric et al., 2000b), these results indicate a correlation between functional receptor expression and cell phenotype differentiation during neural progenitor lineage progression.

emergence of the increasing TuJ1$^+$/BrdU$^-$ cells likely represents continued neuronal cell lineage progression in the 3D collagen gel. To characterize the functional differentiation of entrapped neural progenitors, we tested for the presence of functional neurotransmitter receptors/ion channels using $Ca^{2+}$ imaging. For this analysis, we tested the sensitivity of developing progenitor cells and progeny to ATP, carbachol (CCh), GABA, and glutamate. Cells were incubated in BrdU for 4 h before $Ca^{2+}$ imaging. After imaging, cells were double-immunostained for BrdU and TuJ1, or TuJ1 and GFAP.

We found that cell responses to the neurotransmitters correlated with the lineage progression of collagen-entrapped neural progenitor cells, which are consistent with the emergence and distribution of functional neurotransmitter receptors among neural progenitor cells in vivo (Maric et al., 2000b). Most of collagen-entrapped progeny at day 5 were proliferating and responded to ATP (55%) and/or CCh (89%); about half responded to both CCh and ATP. None of cells at this time responded to GABA or glutamate (Fig. 4a). In contrast, about 60% of progeny at day 14 responded to both GABA and glutamate (Fig. 4b). These GABA- and glutamate-responsive cells were neuron-like in morphology. They were smaller, rounded, and phase-bright, compared to the undifferentiated cells, which were larger and phase-dark. About 38% of the cells still responded to ATP and showed typical undifferentiated cell morphology. This suggests a development-dependent expression of neurotransmitter receptors during neurogenesis, similar to that reported in vivo (Maric et al., 2000b). During the first 2 weeks of

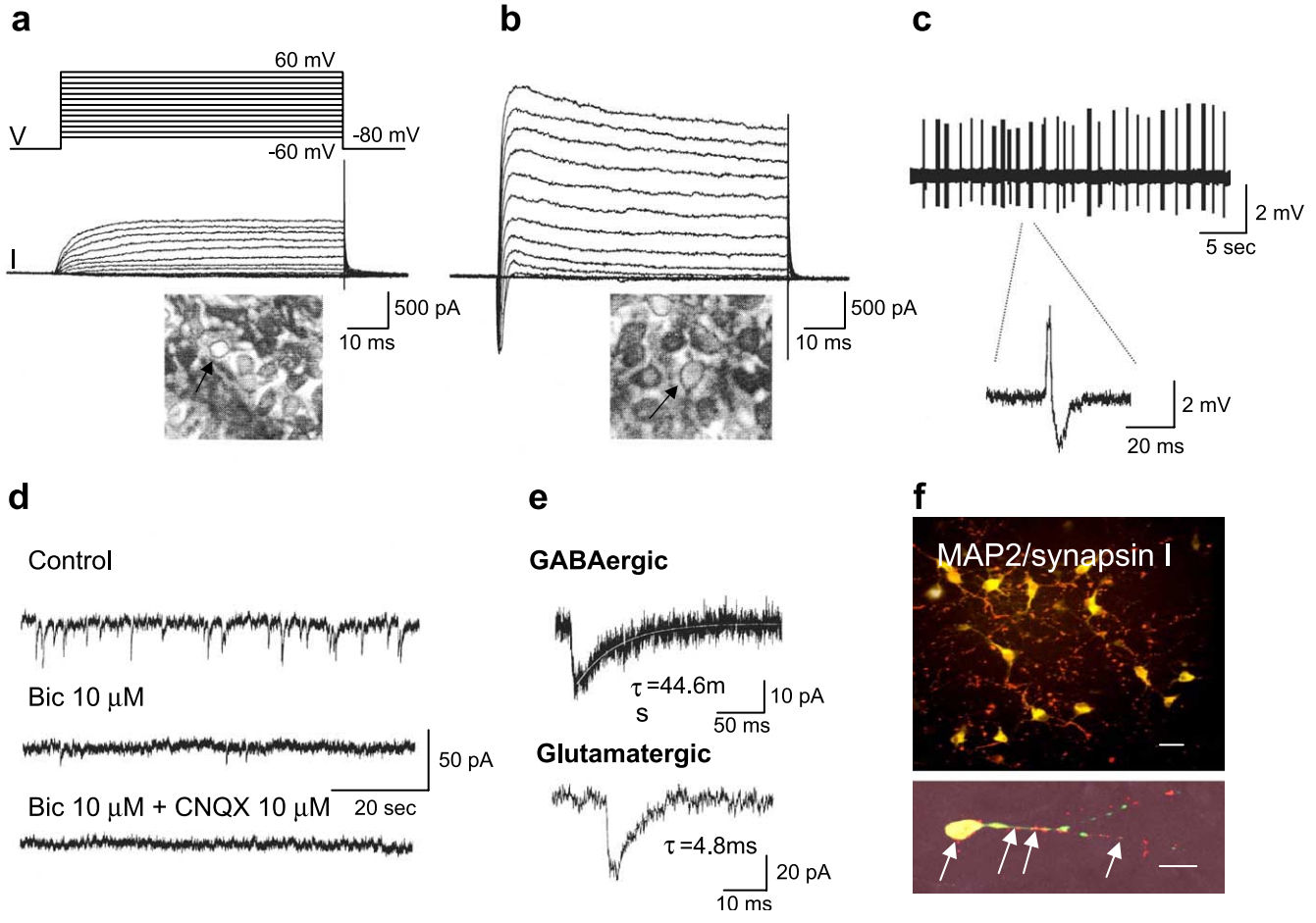


Fig. 5. Electrophysiological properties of neural progenitor cells and their progeny using whole-cell patch clamp recordings of 7-day-old 3D cultures. (a) When 75 ms test pulses from a holding potential of −80 mV to potentials ranging from −60 to 60 mV are applied to neural progenitor cells with an undifferentiated morphology (inset; flat without processes, arrow) only outward $K^+$ currents are recorded. (b) Using the same protocol, cells with neuronal morphology (inset; rounded, phase-bright cell body with long neurites, arrow), both inward $Na^+$ and outward $K^+$ currents are observed. (c) Action potentials are recorded from a cell with neuronal morphology utilizing the fast current-clamp mode of the patch clamp amplifier after polarizing the cell to −60 mV. (d) Spontaneous postsynaptic currents (PSCs) are evident under voltage-clamp at a holding potential of −80 mV (upper trace). Most PSCs are blocked by 10-μM bicuculline, a $GABA_A$ receptor antagonist (middle trace). The remaining PSCs are blocked by 10-μM CNQX, an AMPA receptor antagonist, together with bicuculline (lower trace). (e) The bicuculline-sensitive, GABAergic PSCs decay exponentially with a time constant of 45 ms (upper panel), while the CNQX-sensitive glutamatergic PSCs decay exponentially with a much faster time constant. (f) Double-immunostaining for MAP2 and synapsin I demonstrate a dense network of axons, and dendrites are formed in the collagen gels. The upper panel shows a high density of synapsin I puncta (red) outlining the MAP2$^+$ neuronal cell bodies and dendrites (green-yellow), while the lower panel shows a high magnification of a MAP2$^+$ neuronal cell body with its dendrites surrounded by synapsin I puncta. Scale bars in $f$ = 40 μm.

progenitor cell expansion and differentiation, cell phenotype shifted from mostly proliferating cells to many TuJ1$^+$ cells, which was accompanied with a shift in the expression of functional neurotransmitter receptors from those responding to ATP and CCh to those responding predominantly to GABA and glutamate.

*Voltage-gated ion currents change as neural progenitor cells differentiate in a 3D collagen matrix*

To examine the development of voltage-gated ion currents, we used whole-cell patch clamp techniques to record $K^+$ and $Na^+$ currents from two morphologically distinct populations. The flat phase-dark cells in clone-like clusters appeared to be undifferentiated cells. Voltage-gated outward $K^+$ currents were found in most immature cells without detection of $Na^+$ currents (Fig. 5a). Potassium currents were evoked by 75 ms test pulses from a holding potential of −80 mV to potentials ranging from −60 to 60 mV.

In most recordings, little voltage-gated sodium current was found in undifferentiated cells, but largely found together with potassium currents from cells with phase-bright rounded cell body and long processes characteristic of TuJ1$^+$ neurons (Fig. 5b). Sodium and potassium currents could be consistently evoked by 75 ms steps from a holding potential of −80 mV to test potentials ranging from −60 to 60 mV. With further differentiation, mature neurons had sufficient Na+ currents to generate spontaneous action potentials (see Fig. 5c).

*Progenitor cell-derived neurons generate spontaneous postsynaptic currents (PSCs)*

To examine the excitability and synaptic activity of progenitor cell-derived neurons, patch-clamp recording was performed in morphologically differentiated cells at day 10 in culture. Spontaneous action potentials were recorded from cells with neuronal morphology utilizing the cell-attached patch-clamp method (Fig. 5c). The frequency of spontaneous action potentials varied widely from 0.2 to 5.5 Hz with a mean frequency of 2.9 ± 0.8 Hz ($n = 6$). In whole-cell patch-clamp mode, spontaneous inwardly directed postsynaptic currents were detected under voltage-clamp in four of the cells at a holding potential of −80 mV (Fig. 5d, upper trace). The majority, but not all of the PSCs were blocked by 10-μM bicuculline, a $GABA_A$ receptor antagonist (Fig. 5d, middle trace). The remaining PSCs were blocked by also including 10-μM CNQX, an AMPA type glutamate receptor antagonist (Fig. 5d, lower trace). Therefore, two classes of PSCs were observed. The bicuculline-sensitive, GABAergic PSCs had a decay time constant of approximately 45 ms (upper panel), while the CNQX-sensitive glutamatergic PSCs were an order of magnitude faster with a decay time of approximately 5 ms. These results indicate that the neuronal progeny of the neural precursors have differentiated mechanisms to generate functional synapses.

*Pre- and postsynaptic differentiation*

To examine morphological evidence for synapse formation, double-immunostaining for MAP-2 and synapsin I, which reportedly corresponds to synaptic vesicle clusters within presynaptic specializations, were carried out in 10-day-old cultures after patch clamp recordings and showed that puncta of synapsin I immunoreactivity (red) were

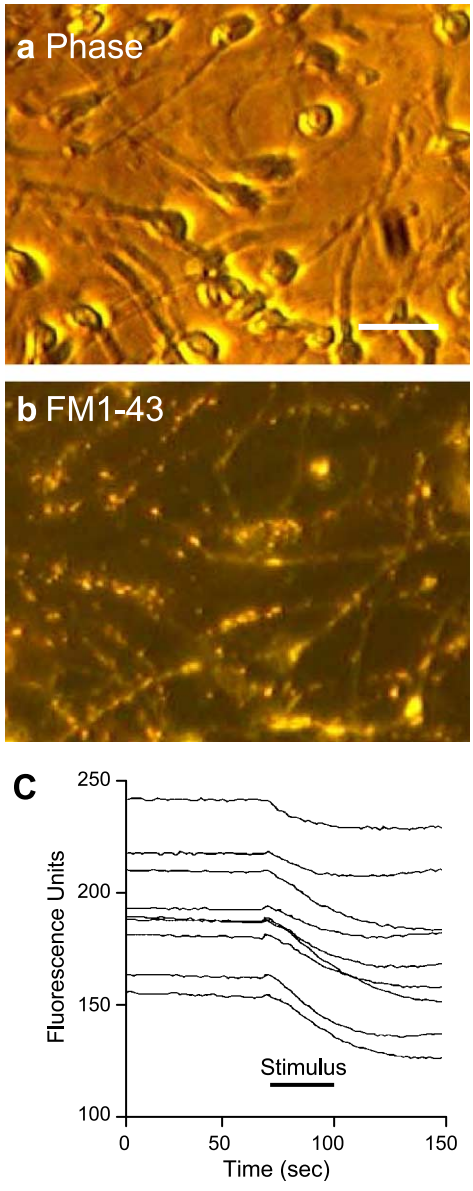


Fig. 6. FM1-43 labeling of recycling synaptic vesicles in collagen-entrapped neurons. Phase-contrast (a) and fluorescent (b) images of the same field of stem cell-derived neurons within collagen gels after loading of FM1−43 in depolarizing extracellular solution. The FM1-43 fluorescent puncta are concentrated at sites where neurites cross over and interact, but cell bodies are not labeled. (c) A subsequent application of depolarizing solution (50 mM $K^+$) without FM1-43 results in a destaining of FM1-43-stained puncta. Changes in FM1-43 fluorescence intensity are recorded from nine FM1-43 loaded sites upon $K^+$ stimulation. The FM1-43 staining is represented by relative fluorescence intensity (fluorescence units). Scale bars in $a = 40$ μm.

abundant and surrounded $MAP2^+$ cell bodies and dendrites (green-yellow) (Fig. 5f). The lower panel shows a high magnification of a $MAP2^+$ neuronal cell body with its dendrites surrounded by synapsin I puncta.

*Developmental maturation of synaptic vesicle cycling in collagen-entrapped neurons*

To test whether the collagen-entrapped neurons develop synaptic activity, cells cultured for 3, 7, 14, and 21 days were loaded with 10-μM FM1-43, which stains recycling synaptic vesicles. Saturating staining was performed using a depolarizing (50 mM $K^+$) extracellular solution to stimulate synaptic vesicle cycling in the presence of FM1-43. This procedure led to a punctuate labeling of functional presynaptic terminals (Figs. 6a, b). FM1-43 fluorescence puncta began to appear in differentiated neurons of day 7 cultures. The intensity of FM1-43 fluorescence increased with time in culture (not shown). This development-dependent fluorescence was concentrated on neurites and sites where neurites crosses over and interacts, but not on cell bodies (Figs. 6a, b). To confirm that fluorescent FM1-43 puncta represent functional synapses, subsequent destaining of dye accumulation was induced by stimulating exocytosis with depolarizing solution in the absence of FM1-43. For quantitative determination of FM1-43 fluorescence changes, 99 sites of interest were recorded using the Zeiss Attofluor Ratio Vision workstation. Fig. 6c shows nine typical individual FM1-43-loaded regions upon stimulation. The decrease in fluorescence was due to fusion of synaptic vesicles with the plasma membrane and the subsequent loss of FM1-43. This result demonstrated synaptic vesicle recycling in collagen-entrapped neurons derived from neural stem and progenitor cells.

## Discussion

A major focus of tissue engineering is to place dissociated cells into synthetic or naturally derived polymer scaffolds in culture. While the creation of many different tissues, including cartilage, tendon, bone, intestine, urinary bladder, and heart valves has been demonstrated using cells and biodegradable polymer scaffolds (Chaignaud et al., 1997), neural tissue engineering has only recently emerged as a strategy for nerve tissue replacement. One of challenges is that neurons cannot proliferate, and neurons in culture are short-lived. Neural stem cells are self-renewing, allowing the ex vivo production of many cells from minimal donor material and providing a virtually unlimited donor source for neural tissue engineering and transplantation. In the present study, cortical and subcortical neuroepithelium is the starting material. It composed of neural stem cells (≤20%) and neuronal and glial progenitors (approximately 80%) (Maric et al., 2003); therefore, the majority of cells in heterogenous unsorted cultures of neuroepithelial cells are progenitors. The neural progenitors have shown their plastic properties based on the ability of neural stem cells to respond to developmental cues. The plasticity can be of advantage in the design of desired neural cell types for tissue reconstruction. The present study has demonstrated that neural progenitor cells dissociated from embryonic cortical and sudcortical regions, and embedded in a 3D collagen gel retain the ability to expand and differentiate into the three lineages comprising neural tissue, including considerable neurons that form functional synapses. In defined medium with bFGF, the progenitor-derived neurons expressed neurotransmitters, neurotransmitter receptors, membrane excitability, and synaptic activity similar to those evolving during CNS development. Thus, cortical and subcortical neural progenitor cells embedded in a 3D collagen gel recapitulate their development in vivo. We conclude that bFGF may synergize with collagen, the major class of insoluble fibrous protein in the extracellular matrix, to induce production of all the lineages that compose CNS tissue and form functional neuronal circuits from neural progenitors.

Many types of tissues, including skin, cornea, mucosal membranes, cartilage, and skeletal tissues have been engineered using stem cells (Bianco and Robey, 2001). Neural progenitor cells were suspended in biodegradable polymer scaffolding materials, particularly hydrogels, and were found to survive and attach to, for example, poly(glycolic acid) (PGA) (Vacanti, 2000). In our previous studies, primary neural stem cells and progenitors were immobilized into 3D collagen gels and the collagen-entrapped cells actively proliferated and differentiated into neurons and astrocytes (O'Connor et al., 2000). The present study extends previous reports and demonstrates the ability of 3D collagen gels to promote neurogenesis from neural stem and progenitor cells and to form neuronal networks through synaptic activity.

Neural progenitor cells cultured in a rotating wall vessel bioreactor were reported to form rudimentary tissue-like structures (Low et al., 2001). The cells were clustered as neurospheres floating in the medium. In the rotating wall vessel bioreactor, cells formed a unique, differentiated structure with a surface layer of proliferating cells that enclosed strata of more differentiated cells within. In our study, neural progenitor cells attached to collagen scaffolds and overtime formed large clusters with a peripheral layer of differentiating $TuJ1^+$ cells that enclosed $BrdU^+$ progenitor cells. This difference in the distribution of differentiating and undifferentiated cells may be due to the fact that neural progenitors need to attach to an ECM for survival and normal development. Collagen as an ECM scaffold has been widely used as a matrix for the growth of a variety of mammalian progenitor cells, including hematopoietic progenitors (Allegraud et al., 1997), mesenchymal stem cells (Butler and Awad, 1999), endothelial cells (Montesano et al., 1983), and neural precursor cells (O'Connor et al., 2000; 2001).

Our studies demonstrate that cells derived from neural progenitor cells exhibit the characteristics of functional neurons in that cells not only show active synaptic vesicle recycling, but also form excitatory and inhibitory connections that generate action potentials spontaneously. Both GABAergic and glutamatergic PSCs were recorded in progenitor-derived functional neuronal circuits. These results are similar to synaptic activity of cortical neurons grown on 3D collagen gels (O'Shaughnessy et al., 2003). The neurotransmitter response profiles of neural progenitors and their progeny was found to shift from widespread responses restricted to only ATP and CCh to responses that also included GABA and glutamate. These results closely parallel the emergence and lineage-restricted distribution of functional receptors occurring in vivo (Maric et al., 2000b). Such progenitor-derived functional neurons may provide a suitable source of cells for neural tissue engineering.

Neural progenitor cells were suspended in biodegradable polymer scaffolding materials, particularly hydrogels, and were found to survive and attach to, for example, poly (glycolic acid) (PGA) (Vacanti, 2000). Hydrogels consist of a 3D polymer network, which swells in water or aqueous media. The viscoelastic nature, high hydration state, and porous form of these polymers have made them useful scaffolds for in vitro and in vivo cellular support (for review, see Woerly et al., 1993). However, neural cells usually do not adhere to synthetic hydrogels because they do not possess receptors for synthetic hydrogels. Therefore, modification of the hydrogels with ECM proteins is necessary to confer biological recognition and cell adhesion. The most abundant ECM proteins in the brain are laminin and fibronectin. A wide range of cell phenotypes, including stem cells (Watt and Hogan, 2000), have been shown to express integrins and focal adhesion kinase (FAK), which plays a central role in integrin-mediated cell adhesion and signal transduction (Ruoslahti, 1997). A more complete understanding of the cell–material interactions and developing bioactive hydrogels for neural progenitor cell growth remain challenges for future studies.

## Acknowledgments

This work was supported in part by NASA grant NRA 00-HEDS-03-136. We thank Kara Shaffer at NRL for her help in preparation of neural progenitor cell dissociates. The opinions and assertions contained herein are the private ones of the authors and are not to be construed as official or reflecting the views of the Department of the Navy.

## References

Allegraud, A., Dobo, I., Praloran, V., 1997. Collagen gel culture of the human hematopoietic progenitors CFU-GM, CFU-E, and BFU-E. Methods Mol. Biol. 75, 221–230.

Bellamkonda, R., Ranieri, J.P., Bouche, N., Aebischer, P., 1998. Hydrogel-based three-dimensional matrix for neural cells. J. Biomed. Mater. Res. 29, 663–671.

Bernhardt, R., Matus, A., 1984. Light and electron microscopic studies of the distribution of microtubule-associated protein 2 in rat brain: a difference between dendritic and axonal cytoskeletons. J. Comp. Neurol. 226, 203–221.

Bianco, P., Robey, P.G., 2001. Stem cells in tissue engineering. Nature 414, 118–121.

Butler, D.L., Awad, H.A., 1999. Perspectives on cell and collagen composites for tendon repair. Clin. Orthop. (367 Suppl.), S324–S332.

Chaignaud, B.G., Langer, B., Vacinti, J.P., 1997. The history of tissue engineering using synthetic biodegradable polymer scaffolds and cells. In: Atala, A., Mooney, D. (Eds.), Synthetic Biodegradable Polymers Scaffolds. Birkhauser Boston, Cambridge, MA.

Fisher, L.J., 1997. Neural precursor cells: applications for the study and repair of the central nervous system. Neurobiol. Dis. 4, 1–22.

Gage, F.H., 1998. Stem cells of the central nervous system. Curr. Opin. Neurobiol. 8, 671–676.

Gage, F.H., 2000. Mammalian neural stem cells. Science 287, 1433–1438.

Gage, F.H., Coates, P.W., Palmer, T.D., 1995. Survival and differentiation of adult neuronal progenitor cells transplanted to the adult brain. Proc. Natl. Acad. Sci. U. S. A. 92, 11879–11883.

Hamill, O.P., Marty, A., Neher, E., Sakmann, B., Sigworth, F.J., 1981. Improved patch-clamp techniques for high-resolution current recording from cells and cell-free membrane patches. Pflugers Arch. 391, 85–100.

Lee, M.K., Tuttle, J.B., Rebhun, L.I., Cleveland, D.W., Frankfurter, A., 1990. The expression and posttranslational modification of a neuron-specific β-tubulin isotope during chick embryogenesis. Cell Motil. Cytoskelet. 17, 118–132.

Lendahl, U., Zimmerman, L.B., McKay, R.D., 1990. CNS stem cells express a new class of intermediate filament protein. Cell 60, 585–595.

Li, B.-S., Ma, W., Zhang, L., Barker, J.L., Stenger, D.A., Pant, H.C., 2001. Activation of phosphatidylinositol-3 kinase (PI-3K) and extracellular kinases (Erk1/2) is involved in muscarinic receptor-mediated DNA synthesis in neural progenitor cells. J. Neurosci. 21, 1569–1579.

Low, H.P., Savarese, T.M., Schwartz, W.J., 2001. Neural precursor cells form rudimentary tissue-like structures in a rotating-wall vessel bioreactor. In Vitro Cell. Dev. Biol., Animal 37, 141–147.

Ma, W., Liu, Q.-Y., Maric, D., Sathanoori, R., Chang, Y., Barker, J.L., 1998. Basic FGF-responsive telencephalic precursor cells express functional $GABA_A$ receptor/$Cl^-$ channels in vitro. J. Neurobiol. 35, 277–286.

Ma, W., Maric, D., Li, B.-S., Andreadis, J.D., Grant, G.M., Liu, Q.-Y., Shaffer, K.M., Chang, Y.-H., Zhang, L., Pancrazio, J., Pant, H.C., Stenger, D.A., Barker, J.L., 2000. Acetylcholine stimulates cortical precursor cell proliferation via muscarinic receptor activation and MAP kinase phosphorylation. Eur. J. Neurosci. 12, 1227–1240.

Maric, D., Liu, Q.-Y., Grant, G.M., Andreadis, J.D., Hu, Q., Chang, Y.C., Barker, J.L., Pancrazio, J.J., Stenger, D.A., Ma, W., 2000a. Functional ionotrophic glutamate receptors emerge during terminal cell division and early neuronal differentiation of rat neuroepithelial cells. J. Neurosci. Res. 61, 652–662.

Maric, D., Maric, I., Chang, Y., Barker, J.L., 2000b. Stereotypical physiological properties emerge during early neuronal and glial lineage development in the embryonic rat neocortex. Cereb. Cortex 10, 729–747.

Maric, D., Maric, I., Chang, Y., Barker, J.L., 2003. Prospective cell sorting of embryonic rat neural stem cells and neuronal and glial progenitors reveals selective effects of basic fibroblast growth factor and epidermal growth factor on self-renewal and differentiation. J. Neurosci. 23, 240–251.

McKay, R.D.G., 1997. Stem cells in the CNS. Science 276, 66–71.

Menezes, J.R.L., Luskin, M.B., 1994. Expression of neuron-specific tubulin defines a novel population in the proliferative layers of the developing telencephalon. J. Neurosci. 14, 5399–5416.

Montesano, R., Mouron, P., Amherdt, M., Orci, L., 1983. Collagen matrix

promotes reorganization of pancreatic endocrine cell monolayers into islet-like organoids. J. Cell Biol. 97, 935–939.
O'Connor, S.M., Stenger, D.A., Shaffer, K.M., Maric, D., Barker, J.L., Ma, W., 2000. Primary neural precursor cell expansion, differentiation and cytosolic $Ca^{2+}$ response in three-dimensional collagen gel. J. Neurosci. Methods 102, 187–195.
O'Connor, S.M., Stenger, D.A., Shaffer, K.M., Ma, W., 2001. Survival and neurite outgrowth of rat cortical neurons in three-dimensional agarose and collagen gel matrices. Neurosci. Lett. 304, 189–193.
O'Shaughnessy, T.J., Lin, H.J., Ma, W., 2003. Functional synapse formation among rat cortical neurons grown on three-dimensional collagen gels. Neurosci. Lett. 340, 169–172.
Ruoslahti, E., 1997. Stretching is good for a cell. Science 276, 1345–1346.
Stenger, D.A., Hickman, J.J., Bateman, K.E., Ravenscroft, M.S., Ma, W., Pancrazio, J.J., Shaffer, K., Schaffner, A.E., Cribbs, D.H., Cotman, C.W., 1998. Microlithographic determination of axonal/dendritic polarity in cultured hippocampal neurons. J. Neurosci. Methods 82, 167–173.
Vacanti, M.P., 2000. Neural Stem Cells. In: Lanza, R.P., Langer, R., Vacanti, J. (Eds.), Principles of Tissue Engineering, second ed. Academic Press, San Diego, pp. 821–830.
Watt, F.M., Hogan, B.L.M., 2000. Out of Eden: stem cells and their niches. Science 287, 1427–1430.
Woerly, S., Maghami, G., Duncan, R., Subr, V., Ulbrich, K., 1993. Synthetic polymer derivatives as substrata for neuronal adhesion and growth. Brain Res. Bull. 30, 415–422.
Woerly, S., Petrov, P., Sykova, E., Roitbak, T., Simonova, Z., Harvey, A.R., 1999. Neural tissue formation within porous hydrogels implanted in brain and spinal cord lesions: ultrastructural, immunohistochemical, and diffusion studies. Tissue Eng. 5, 469–488.